applied sciences

MDPI

Article

Effect of Impeller Trimming on the Energy Efficiency of the Counter-Rotating Pumping Stage

Ivan Pavlenko [1,2], Oleksandr Kulikov [3], Oleksandr Ratushnyi [3], Vitalii Ivanov [1,4], Ján Piteľ [1,*] and Vladyslav Kondus [3,5]

[1] Faculty of Manufacturing Technologies with a Seat in Presov, Technical University of Kosice, Bayerova 1, 080 01 Presov, Slovakia
[2] Department of Computational Mechanics Named after Volodymyr Martsynkovskyy, Faculty of Technical Systems and Energy Efficient Technologies, Sumy State University, 2, Rymskogo-Korsakova St., 40007 Sumy, Ukraine
[3] Department of Applied Hydro- and Aeromechanics, Faculty of Technical Systems and Energy Efficient Technologies, Sumy State University, 2, Rymskogo-Korsakova St., 40007 Sumy, Ukraine
[4] Department of Manufacturing Engineering, Machines and Tools, Faculty of Technical Systems and Energy Efficient Technologies, Sumy State University, 2, Rymskogo-Korsakova St., 40007 Sumy, Ukraine
[5] Sumy Machine-Building Cluster of Energy Equipment, Sumy State University, 2, Rymskogo-Korsakova St., 40007 Sumy, Ukraine
* Correspondence: jan.pitel@tuke.sk

Abstract: Developing ways to increase centrifugal pumps' pressure and power characteristics is a critical problem in up-to-date engineering. There are many ways to resolve it, but each has advantages and flaws. The presented article aimed to ensure higher energy efficiency indicators by using a counter-rotating pumping stage with trimming. During the research, the comprehensive approach was based on CFD modeling and the Moore–Penrose pseudoinverse approach for overestimated systems. According to the obtained data, pumps with a counter-rotating stage allowed the pressure head to be significantly increased compared with the standard design of the flow part. Notably, for pumping units CPS 180/1900 with a basic stage, the pressure head of 127 m was reached. However, when using a counter-rotating stage, the pressure head could be increased up to 270 m, which was 2.1 times higher. Therefore, to ensure unchanged characteristics when using centrifugal pumps with the counter-rotating stage, the weight and size indicators can be significantly reduced compared to the traditional design scheme. The proposed numerical and analytical approaches allow estimating the highest pressure and energy characteristics values.

Keywords: energy efficiency; centrifugal pump; power consumption; process innovation

Citation: Pavlenko, I.; Kulikov, O.; Ratushnyi, O.; Ivanov, V.; Piteľ, J.; Kondus, V. Effect of Impeller Trimming on the Energy Efficiency of the Counter-Rotating Pumping Stage. *Appl. Sci.* **2023**, *13*, 761. https://doi.org/10.3390/app13020761

Academic Editor: Joon Ahn

Received: 6 December 2022
Revised: 28 December 2022
Accepted: 3 January 2023
Published: 5 January 2023

1. Introduction

Impeller trimming is widely used when adjusting centrifugal pumps and expanding their application area [1]. Trimming the impeller along the outer diameter by 10–15% is permitted so as to change parameters and sequential operation of a couple of pumps.

One of the most affordable ways is to trim the impeller along the outer diameter [2]. Many studies have been devoted to this issue, the essence of which is to obtain experimental coefficients for calculating the pressure head, hydraulic losses, and energy efficiency depending on the trimming value. However, each type of pump requires different experiments to be carried out.

When using a counter-rotating stage, the main pressure head is created due to the negative swirl of the flow, which is itself created when the liquid leaves the impeller and enters the vane disk [3]. In this case, the primary characteristic is not the speed of the liquid flow, but the angle of its inflow to the entrance to the vane disk.

Impeller trimming changes the impeller's overall dimensions and the liquid outlet's angle. This fact affects the pressure head, power consumption, and energy characteristics of the counter-rotating stage.

Impeller trimming has been thoroughly investigated for standard impellers. However, the effect of impeller trimming on the counter-rotating stage is unknown. This is because transferring energy to the liquid in a counter-rotating stage is highly complicated.

Various researchers worldwide have highlighted the significance of the stated problem in ensuring the energy efficiency of centrifugal pumps. Li [4] studied the impeller trimming of an industrial centrifugal viscous oil pump, and the effect of increasing efficiency was revealed when a trimmed impeller delivered highly viscous oils. Detert Oude Weme et al. [5] proposed an algorithm for the prediction of the effect of impeller trimming on the hydraulic performance of low specific-speed centrifugal pumps. The proposed approach overestimated the reduction in the pressure head after trimming.

Khoeini and Tavakoli [6] evaluated the flow characteristics of a centrifugal pump with different impeller trimming methods. They showed that the efficiency of a polygon-shaped trimmed impeller was less than the best efficiency point. Deng et al. [7] studied the effect of impeller trimming on performance in a double-suction centrifugal pump. The losses in the volute diffuser channel were substantiated by the vortices generated within flow separation and backflow. Radial force variation caused by impeller trimming in the double-suction centrifugal pump was also investigated in [8].

Moreover, many research tasks concerning impeller trimming are also essential for compressors, turbines, and fans. Swain and Engeda [9] studied the performance impact of impeller blade trimming on centrifugal compressors. They proved that blade trimming could be applied to reduce the pressure ratio while maintaining flow range. Jawad et al. [10] also investigated the effect of impeller trimming on the performance of a modified compressor using a numerical simulation approach.

Yang et al. [11] conducted experimental research on a single stage regarding the effects of impeller trimming for a turbine. The influence of parallel impeller inlet trimming on a mixed flow pump as a turbine was studied in [12]. Wang et al. [13] experimentally and numerically investigated the effect of blade trimming on squirrel cage fan aerodynamic performance. Li et al. [14] numerically studied the impeller trimming effect on the performance of an axial flow fan, and Ye et al. [15] analyzed the performance of the axial fan after blade trimming.

Moreover, Shi et al. [16] provided an experimental and numerical analysis of combined hydrogen as a combustion enhancer applied to the Wankel engine. The design of this pump is based on a dynamic type of energy transfer. Simultaneously, the Wankel engine is based on the rotary–piston principle of energy transfer, or positive displacement engines. They also clarified the role of turbulence-induced blade configuration in improving rotary engines [17]. The implementation of various bowl designs in an HPDI natural gas engine, focused on performance and pollutant emissions, was presented in [18].

After considering all the above, the following problems can be formulated. The effect of impeller trimming on the counter-rotating stage should be investigated. There are still no analytical formulae for calculations. However, such an energy transfer requires thorough study. This is because it can clarify the pump's operation principle for counter-rotating stages.

This study aimed to analyze the energy efficiency of a counter-rotating stage of centrifugal pumps by impeller trimming. To achieve this goal, the following objectives were formulated. Firstly, hydrodynamic processes in the counter-rotating stage of a centrifugal pump were studied. Secondly, various types of impellers for the counter-rotating stage under impeller trimming were designed. A numerical study of the flow parts using the proposed changes was carried out by means of numerical simulation. Finally, an approximation of the obtained pressure and energy characteristics for the trimming range up to 25 mm were realized.

In this regard, a couple of case studies were considered. The first impeller type had a blade disk that lengthened when the trimming increased. The overall size of this blade disk remained unchanged. However, the second type had a constant height. In this case, the overall size decreased as the trimming increased.

2. Materials and Methods

2.1. Fundamental Criteria

Trimming the outer diameter of the impeller increases the gap between the impeller and the spiral guide vane. As a result, equalization of the flow behind the centrifugal wheel decreases the force interaction of the flow with the working parts of the impeller. This effect is widely used to reduce pressure pulsations, vortices, and noise of the pumping unit [19].

When reducing the output diameter D_2 of an impeller, peripheral speed decreases. Therefore, the pressure head of the centrifugal stage is decreased. Experiments show that moderate impeller trimming slightly changes the pump's energy efficiency.

When impeller trimming for centrifugal pumps, the impeller correction and the change in pump characteristics can be roughly determined by the following similarity equations [20]:

$$Q' = Q\frac{D_2'}{D_2};\ H' = H\left(\frac{D_2'}{D_2}\right)^2;\ N' = N\left(\frac{D_2'}{D_2}\right)^3, \quad (1)$$

where Q, H, N, D_2 represents the nominal flow rate [m^3/h], pressure head [m], power consumption [kW], and external diameter of the impeller [m] before trimming; Q', H', N', and D_2' represents the nominal flow rate [m^3/h], pressure head [m], power consumption [kW], and external diameter of the impeller [m] after trimming.

These dependencies allow the building of the characteristics of a pump with a turned wheel. Remarkably, the impeller turning along the outer diameter changes not only the pump's characteristics but also its speed ratio:

$$n_s = 3.65n\frac{\sqrt{Q}}{\sqrt[4]{H^3}}, \quad (2)$$

where n—operating speed, rpm.

Simultaneously, the pressure head decreased more significantly than that according to the standard calculation technique. The energy efficiency of the pump decreased too. Consequently, the rational impeller trimming should be consistent with the speed ratio.

2.2. The Counter-Rotating Stage

In regard to the counter-rotating effect, for ease of perception, the gratings were spaced at a certain distance a (Figure 1).

Velocity vectors and their components are presented for an axisymmetric flow mode. The following condition is also met: grids rotate in opposite directions with the same angular velocity:

$$\omega_I = -\omega_{II}, \quad (3)$$

where ω_I, ω_{II}—rotation speed of the first and second grids, respectively, rad/s.

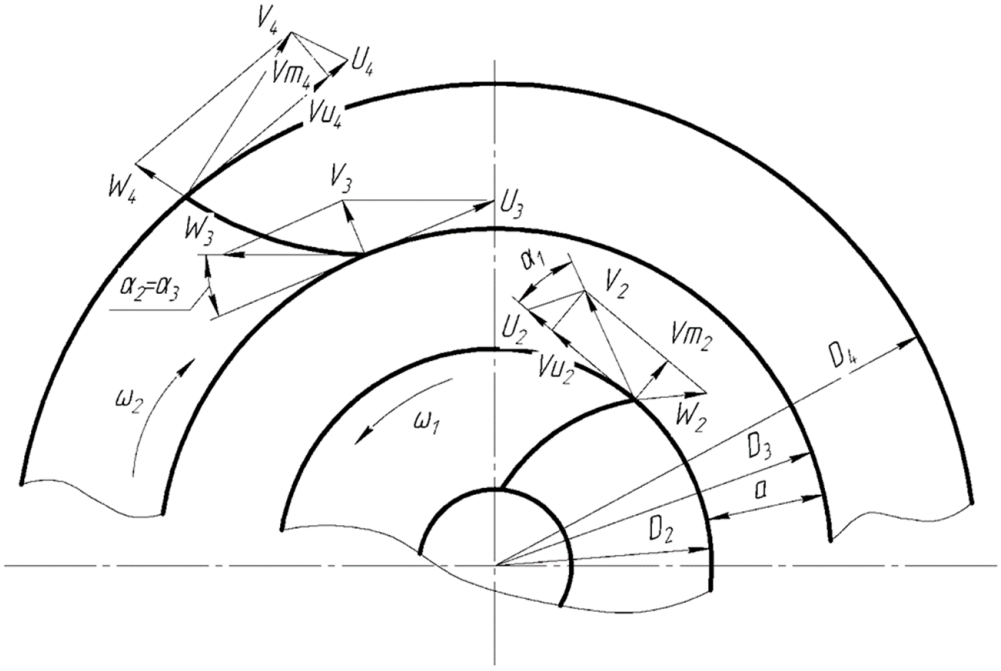

Figure 1. Flow kinematics in a centrifugal counter-rotating stage.

Moreover, non-circulating inflow conditions were chosen at the inlet to each grid. Simultaneously, if this condition was easy to satisfy for the first lattice (v_{u1} = 0) due to the feeder design, the condition of v_{u3} = 0 was more difficult to ensure at the inlet to the second grid. This could be achieved only due to the appropriate geometric and kinematic parameters of both the first and second grids.

At the inlet to the second grid, the liquid has a significant momentum $v_{u2} \cdot r_2$, created by the first lattice. Simultaneously, its direction is opposite to the rotating direction of the second grid. Although the vector v_3 does not create whirl (v_{u3} = 0), the whirl $v_{u2} \cdot r_2$ is the negative circulation at the entrance to the second grid [21].

The blades of the second grid move towards the flow coming out from the first one, changing its momentum rapidly. According to the momentum theorem [22], this causes a sharp increase in the force of interaction between the blade and the fluid flow. This leads to a significant increase in the intensity of the energy transfer process.

Therefore, the flow at the inlet to the second grid with a significant negative circulation provides an intense counterflow for the blades of the second part of the counter-rotating stage [23]. Consequently, the kinetic energy of this flow changes into the potential energy of the pressure head, like jet turbines.

2.3. Mathematical Modeling

Analytical studies were carried out under the same conditions for trimming t in a range from t_0 [mm] to t_1 [mm] with a certain step $\Delta t = (t_1 - t_0)/n_t$ [mm], where n_t—the total number of trimming modes. These values allowed obtaining the pressure and energy characteristics of the counter-rotating stage with an arbitrary value of the impeller trimming. For this purpose, the quadratic approximation was applied:

$$\begin{Bmatrix} H(t) \\ N(t) \\ \eta(t) \end{Bmatrix} = \begin{bmatrix} K_{11} & K_{12} & K_{13} \\ K_{21} & K_{22} & K_{23} \\ K_{31} & K_{32} & K_{33} \end{bmatrix} \begin{Bmatrix} 1 \\ t \\ t^2 \end{Bmatrix}, \quad (4)$$

where t—trimming, mm; H—pressure head, m; N—power consumption, kW; η—energy efficiency, %; [K]—compliance matrix.

The physical meaning of the coefficients of the matrix [K] follow:. coefficients $K_{11} = H(0)$, $K_{21} = N(0)$, and $K_{31} = \eta(0)$ are pressure head, power consumption, and energy efficiency for an impeller without trimming. They equal the initial values of the curves $H(t)$, $N(t)$, and $\eta(t)$, respectively.

Parameters $K_{12} = dH(0)/dt$, $K_{22} = dN(0)/dt$, and $K_{32} = d\eta(0)/dt$ are the 1st time derivatives of these values for an impeller without trimming. They reflect the initial slope angle of the curves $H(t)$, $N(t)$, and $\eta(t)$. If these parameters are positive, the curve initially ascends and if they are negative it descends.

Finally, parameters $K_{13} = 0.5\, d^2H(0)/dt^2$, $K_{23} = 0.5\, d^2N(0)/dt^2$, and $K_{33} = 0.5\, d^2\eta(0)/dt^2$ equal half of the 2nd time derivatives of the pressure head, power consumption, and energy efficiency, respectively. They reflect the curvature of the curves $H(t)$, $N(t)$, and $\eta(t)$. Moreover, if these parameters are positive, the curvature is concave and if negative it is convex.

The unknown elements of the matrix [K] can be evaluated based on the following matrix equation:

$$[T]\begin{Bmatrix} K_{11} \\ K_{12} \\ K_{13} \end{Bmatrix} = \begin{Bmatrix} H_0 \\ \dots \\ H_1 \end{Bmatrix};\ [T]\begin{Bmatrix} K_{21} \\ K_{22} \\ K_{23} \end{Bmatrix} = \begin{Bmatrix} N_0 \\ \dots \\ N_1 \end{Bmatrix};\ [T]\begin{Bmatrix} K_{31} \\ K_{32} \\ K_{33} \end{Bmatrix} = \begin{Bmatrix} \eta_0 \\ \dots \\ \eta_1 \end{Bmatrix} \tag{5}$$

where $H_0, \dots, H_1$—a range of pressure heads for various trimmings t; [T]—3 × 3 matrix of trimming coefficients:

$$[T] = \begin{bmatrix} 1 & t_0 & t_0^2 \\ \dots & \dots & \dots \\ 1 & t_1 & t_1^2 \end{bmatrix}. \tag{6}$$

Since the total number of experimental points can be more than the total number of evaluated parameters, the regression analysis for an overdetermined system (5) should be applied. As a result, the following linear regression dependencies allow for estimating of the unknown elements of the matrix [K]:

$$\begin{Bmatrix} K_{11} \\ K_{12} \\ K_{13} \end{Bmatrix} = [\Theta]\begin{Bmatrix} H_0 \\ \dots \\ H_1 \end{Bmatrix};\ \begin{Bmatrix} K_{21} \\ K_{22} \\ K_{23} \end{Bmatrix} = [\Theta]\begin{Bmatrix} N_0 \\ \dots \\ N_1 \end{Bmatrix};\ \begin{Bmatrix} K_{31} \\ K_{32} \\ K_{33} \end{Bmatrix} = [\Theta]\begin{Bmatrix} \eta_0 \\ \dots \\ \eta_1 \end{Bmatrix}, \tag{7}$$

where [Θ], the Moore–Penrose pseudoinverse matrix [24] is:

$$[\Theta] = \left([T]^T[T]\right)^{-1}[T]^T. \tag{8}$$

Formula (4) allows determining of the extremum values of pressure head, power consumption, and energy efficiency according to the following expressions:

$$\frac{d}{dt}\begin{Bmatrix} H(t) \\ N(t) \\ \eta(t) \end{Bmatrix} = \begin{Bmatrix} K_{12} + 2K_{13}t^* \\ K_{12} + 2K_{13}t^{**} \\ K_{12} + 2K_{13}t^{***} \end{Bmatrix} = \{0\}, \tag{9}$$

where {0}—3 × 1 zero column-vector; t^*, t^{**}, and t^{***}—trimming values, leading to the extremum of pressure head, power consumption, and energy efficiency, respectively:

$$t^* = -\frac{K_{12}}{2K_{13}};\ t^{**} = -\frac{K_{22}}{2K_{23}};\ t^{***} = -\frac{K_{32}}{2K_{33}}. \tag{10}$$

After the substitution of expression (10) to Formula (4) and consequent equal algebraic transformations, the corresponding extremum values are as follows:

$$H(t^*) = K_{11} - \frac{K_{12}^2}{4K_{13}};\ N(t^{**}) = K_{21} - \frac{K_{22}^2}{4K_{23}};\eta(t^{***}) = K_{31} - \frac{K_{32}^2}{4K_{33}}. \tag{11}$$

Remarkably, the consequence of dependencies (4)–(11) is the same for the elongated and replaced counter-rotating stages.

Moreover, Formula (4) allows evaluation of the trimming values t_*, t_{**}, and t_{***}, when the pressure head, power consumption, and energy efficiency are the same as for the impeller without trimming:

$$\begin{Bmatrix} H(t_*) \\ N(t_{**}) \\ \eta(t_{***}) \end{Bmatrix} = \begin{Bmatrix} K_{11} + K_{12}t_* + K_{13}t_*^2 \\ K_{21} + K_{22}t_{**} + K_{23}t_{**}^2 \\ K_{31} + K_{32}t_{***} + K_{33}t_{***}^2 \end{Bmatrix} = \begin{Bmatrix} H(0) \\ N(0) \\ \eta(0) \end{Bmatrix}. \quad (12)$$

It can be substantiated, after solving the corresponding quadratic equations, that the pressure and energy parameters of the trimmed impeller are the same at trimming values twice those for the extremum values: $t_* = 2t^*$, $t_{**} = 2t^{**}$, and $t_{***} = 2t^{***}$.

3. Results

3.1. Design Models

The object of the study was a counter-rotating stage for a basic pump CPS-180/1900. The counter-rotating stage consists of an impeller *I* and blade disk *II* (Figure 2).

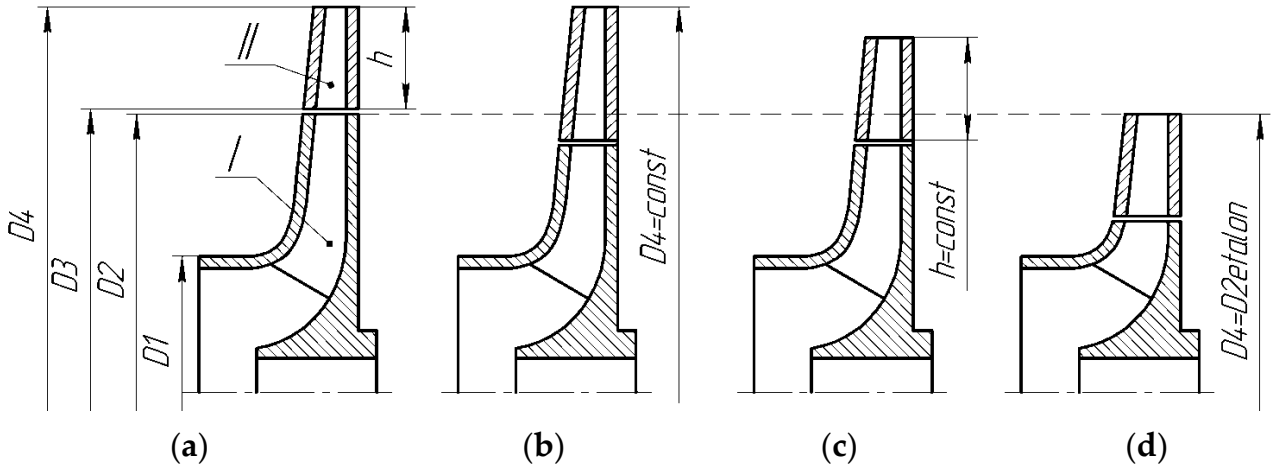

Figure 2. Counter-rotating stages: (**a**) Reference stage; (**b**) The elongated counter-rotating stage (D_4 = constant); (**c**) The replaced counter-rotating stage (h = constant); (**d**) The diameter D_4 of the counter-rotating stage equals to the diameter D_2 of the impeller for the reference stage.

A counter-rotating stage without trimming was also considered as a reference stage (Figure 2a), with which other results for four impellers, trimmed by 5, 10, 15, and 20 mm, were compared.

The following different types of studies were realized. In the first case study, the outer diameter D_4 of the blade disk was constant (Figure 2b). In the second one, the height h of the blade disk was constant (Figure 2c). The last case study was carried out for an impeller with trimming of 52 mm under the condition that the largest size D_4 of the counter-rotating stage was equal to the size D_2 of the reference impeller (Figure 2d).

Geometric dimensions of the reference counter-rotating stage (without trimming) were as follows: the outer diameter of the impeller—D_2 = 302 mm; the outer diameter of the blade disk—D_4 = 410 mm; the gap between the working elements of the step—2 mm; the blade disk height—h = 52 mm.

3.2. CFD Modeling

Initially, impellers with different outer diameters D_2 were designed (Figure 3a). For each impeller, two different vane disks were created using the Solid Works software.

Using the ANSYS CFX software [25], the 3D models were meshed by the calculation grid (Figure 3b).

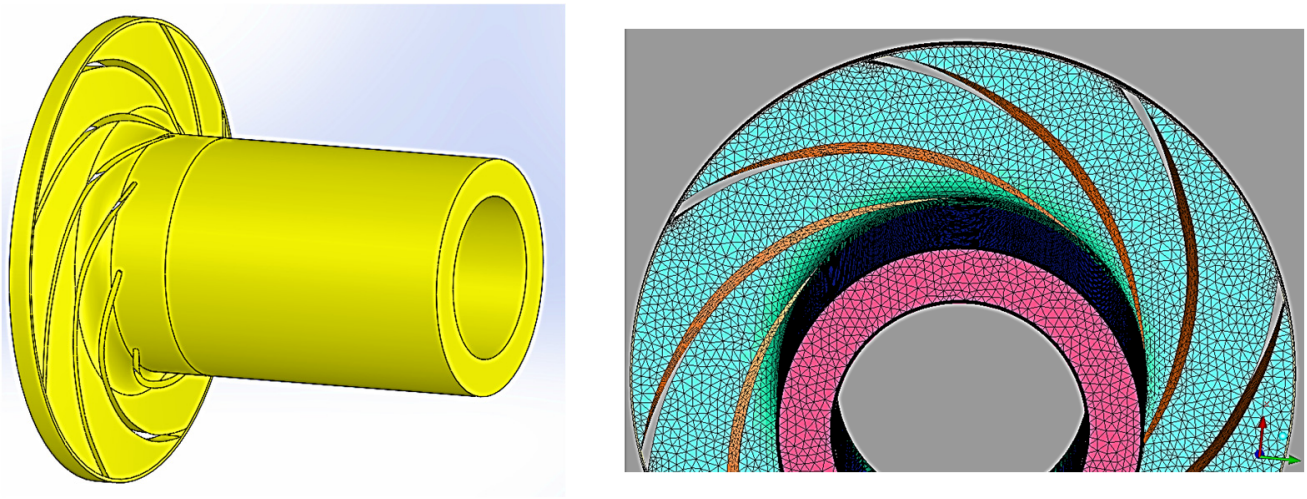

(**a**) (**b**)

Figure 3. 3D model (**a**) and CFD grid (**b**) of the flow part.

Grid independence allowed obtaining high-quality numerical simulation by determining the optimal cell size of the grid for further calculations. During the grid independence test, it was determined that the global mesh size of the cells equaled 7 mm. The number of prismatic layers should be at least 11. Moreover, the first layer should be 0.04 mm. Overall, on average, the number of cells in the grid was 1.5×10^6.

The next stage for each model was the "inlet" and "outlet" conditions, setting of the pumped medium and specific boundary conditions. After that, the numerical calculations of counter-rotating stages were carried out.

Initially, counter-rotating stages with different trimming values and bladed disks were calculated. The first study concerned impeller trimming by 5 mm (Figure 4).

Two counter-rotating systems were designed and simulated for this case study (and subsequent case studies). The first system considered the elongated counter-rotating stage (Figure 4a) with D_4 = constant. The second system considered the replaced counter-rotating stage (Figure 4b) with h = constant.

The characteristics of these degrees were as follows: the first option (D_4 = constant)—pressure head H = 411 m, power consumption N = 400 kW, and energy efficiency η = 50%; the second option (h = constant)—H = 396 m, N = 391 kW, and η = 49%.

In the designed stages, vortex formation occurs due to the sizeable inter-blade channel. Traditionally, such vortices negatively impact the pressure and energy characteristics. However, in the considered case study, vortex formation did not have an effect because of the similar parameters for all the stages (number of blades, their shape and thickness, and blade angle).

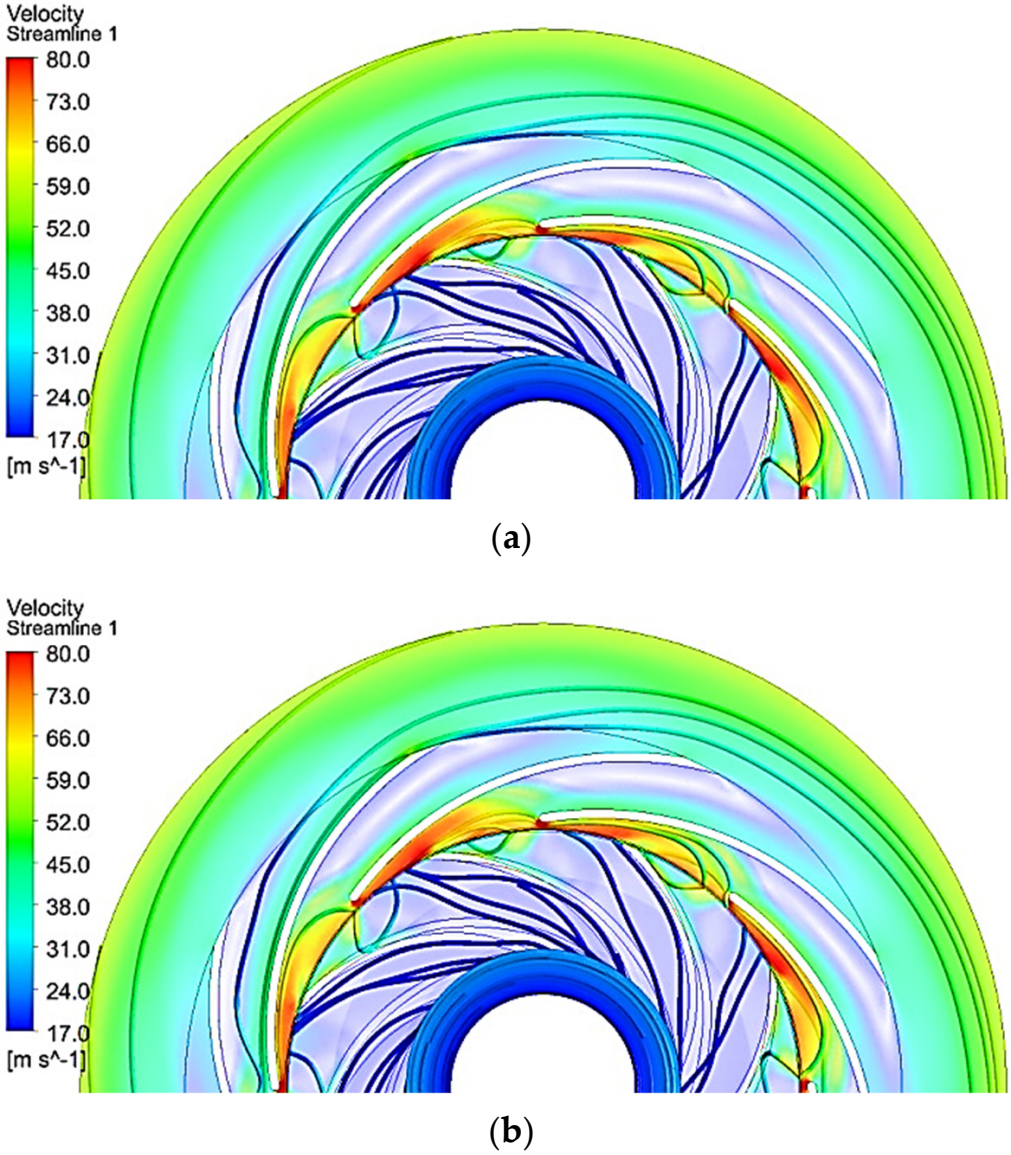

Figure 4. Stages with trimming of 5 mm: (**a**) D_4 = constant; (**b**) h = constant.

The next step was the calculation of counter-rotating stages with various impeller trimmings of 10 mm (Figure 5). The characteristics of these degrees were as follows: the first option (D_4 = constant)—H = 431 m, N = 408 kW, and η = 52%; the second option (h = constant)—H = 392 m, N = 382 kW, η = 50%.

Next, counter-rotating stages with different impeller trimmings of 15 mm were calculated (Figure 6). The characteristics of these degrees were as follows: the first option (D_4 = constant)—H = 407 m, N = 344 kW, and η = 58%; the second option (h = constant)—H = 364 m, N = 313 kW, and η = 54%.

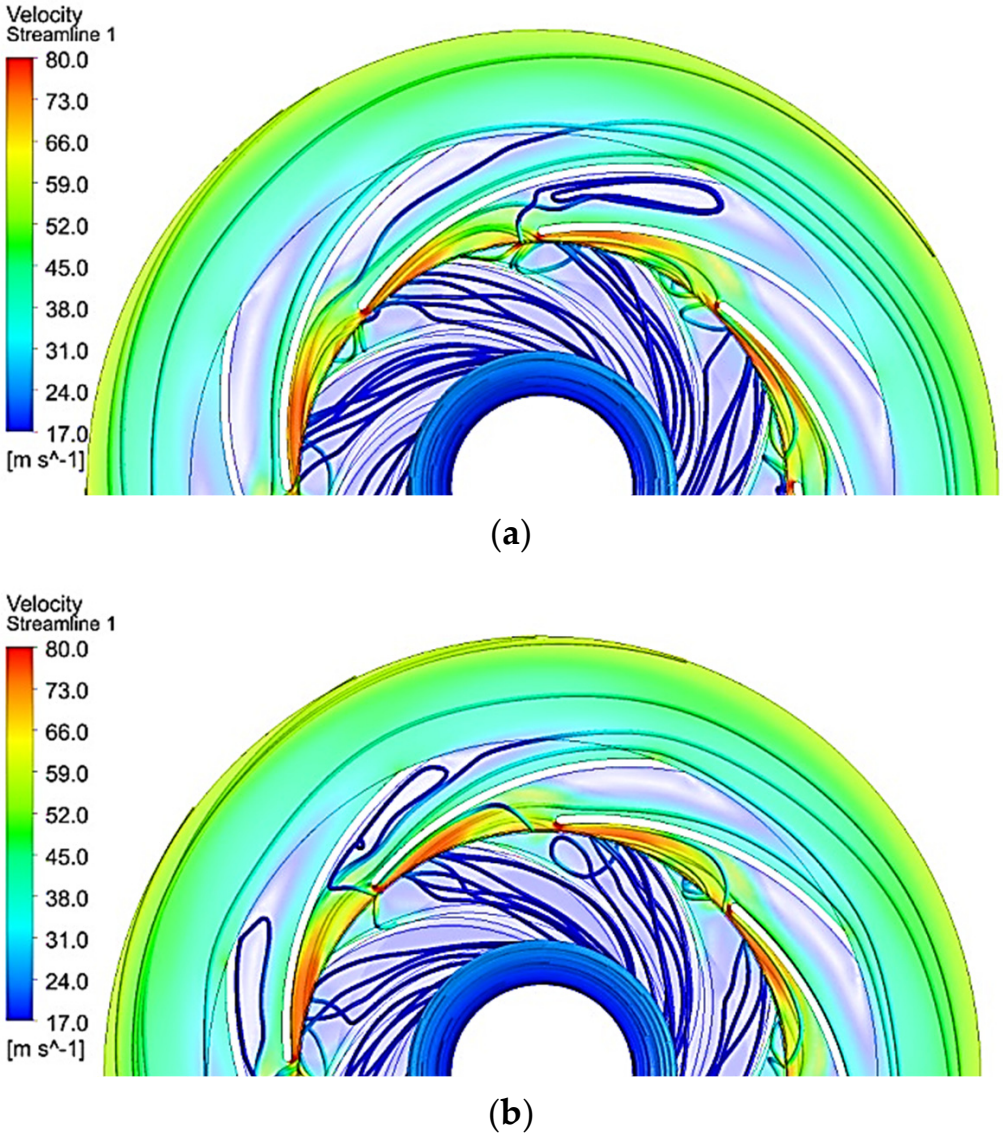

Figure 5. Stages with trimming of 10 mm: (**a**) D_4 = constant; (**b**) h = constant.

The last step was the calculation of counter-rotating stages with various trimmings of 20 mm (Figure 7). The characteristics of these degrees were as follows: the first option (D_4 = constant)—H = 348 m, N = 282 kW, and η = 60%; the second option (h = constant)—H = 276 m, N = 241 kW, and η = 65%.

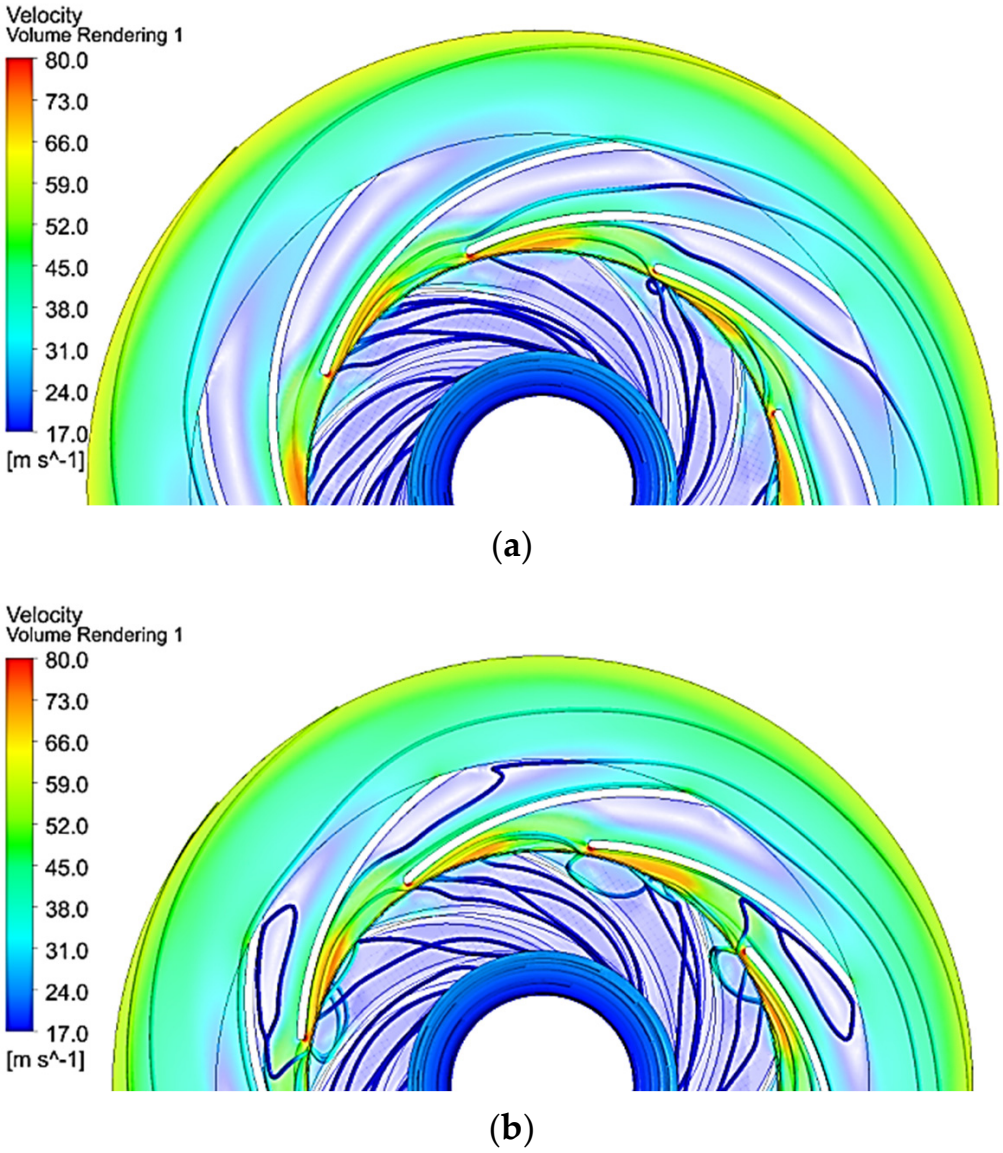

Figure 6. Stages with trimming of 15 mm: (**a**) D_4 = constant; (**b**) h = constant.

To compare the pressure and energy characteristics, the reference counter-rotating stage was also calculated (Figure 8a). Additionally, the influence of the maximally trimmed impeller of the counter-rotating step with overall dimensions less than for a reference impeller of the pump CPS-180/1900 was studied (Figure 8b).

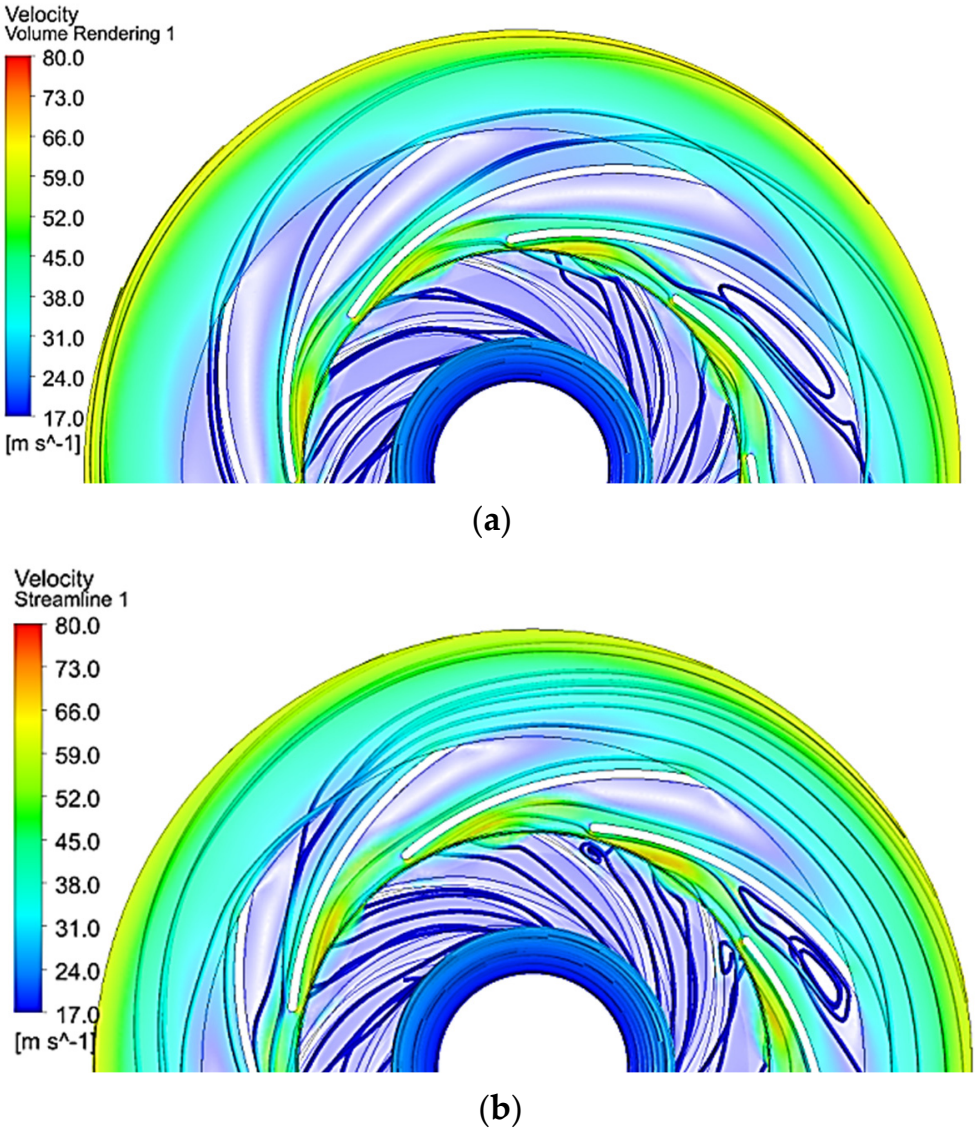

Figure 7. Stages with trimming of 20 mm: (**a**) D_4 = constant; (**b**) h = constant.

The characteristics of these degrees were as follows: without trimming—H = 387 m, N = 331 kW, and η = 57%; after trimming of 52 mm—H = 184 m, N = 139 kW, and η = 65%.

Thus, the impeller trimming significantly affected the pressure and energy characteristics of the counter-rotating stages of the centrifugal pump.

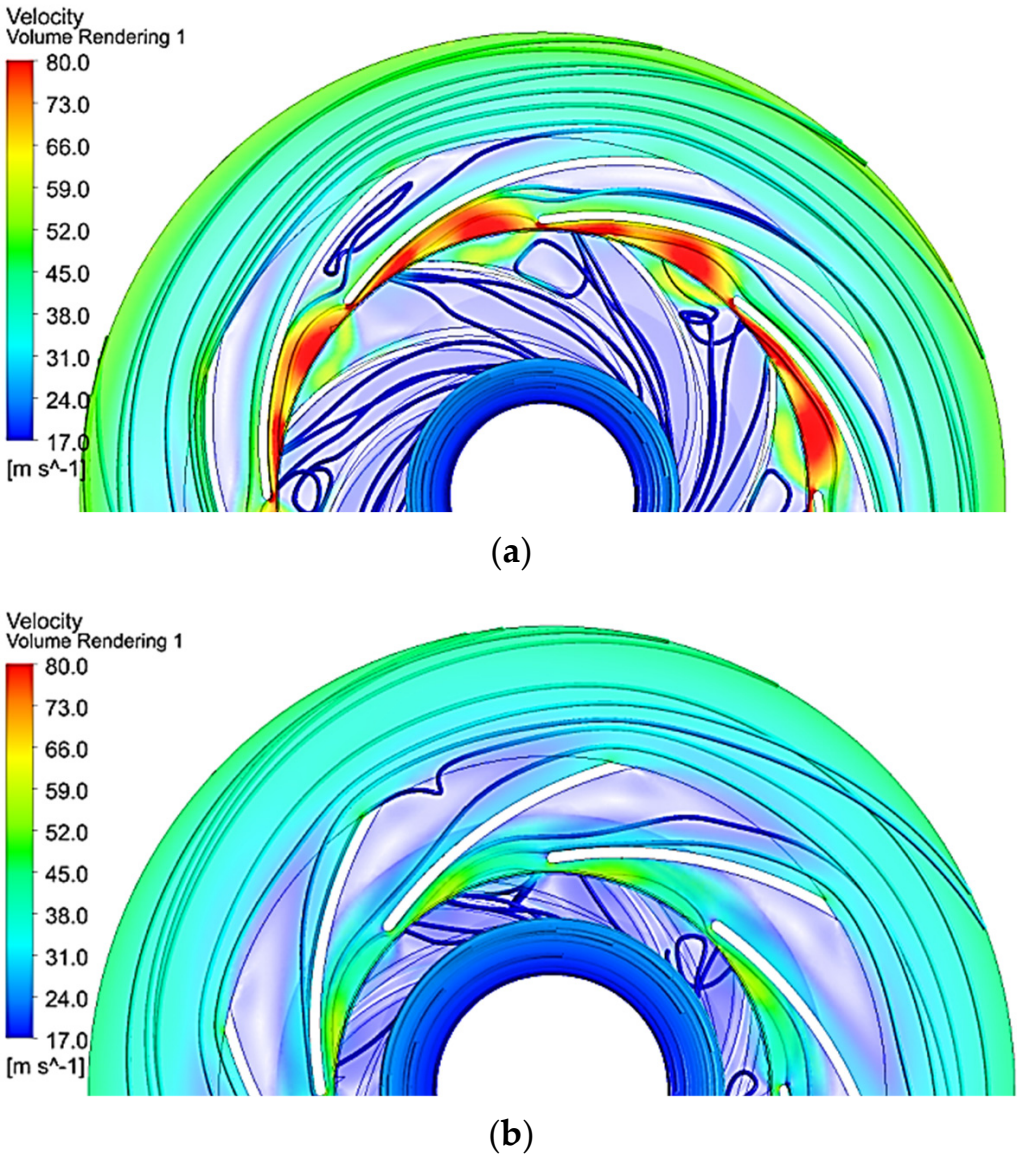

Figure 8. Counter-rotating stages: (**a**) reference (without trimming); (**b**) with trimming of 52 mm.

3.3. Overall Evaluation Results

All the obtained data after the CFD simulations are summarized in Table 1.

Table 1. Pressure and energy characteristics of counter-rotating stages for different trimming modes.

Trimming Value, mm	D_4 = Const			h = Const		
	Pressure Head H, m	Power Consumption N, kW	Energy Efficiency, kW	Pressure Head H, m	Power Consumption N, kW	Energy Efficiency, kW
0 *	387	331	57	387	331	57
5	411	400	50	396	391	49
10	431	408	52	392	382	50
15	407	344	58	346	313	54
20	348	282	60	276	241	65
25	n/a	n/a	n/a	184	139	65

* without trimming; n/a—not allowed.

The following data were evaluated as a result of applying the mathematical model (4)–(8). Firstly, for the elongated counter-rotating stage (D_4 = const), the matrix of trimming

coefficients [T] (6), the Moore–Penrose pseudoinverse matrix [Θ] (8), and the compliance matrix [K] (7) were as follows:

$$[T] = \begin{bmatrix} 1 & 0 & 0 \\ 1 & 5 & 25 \\ 1 & 10 & 100 \\ 1 & 15 & 225 \\ 1 & 20 & 400 \end{bmatrix}; [\Theta] = \begin{bmatrix} 0.886 & 0.257 & -0.086 & -0.143 & 0.086 \\ -0.154 & 0.037 & 0.114 & 0.077 & -0.074 \\ 0.006 & -0.003 & -0.006 & -0.003 & 0.006 \end{bmatrix};$$

$$[K] = \begin{bmatrix} 383.2 & 10.36 & -0.6 \\ 336.086 & 16.006 & -0.954 \\ 55.743 & -0.977 & 0.063 \end{bmatrix}.$$

However, for the replaced counter-rotating stage (h = const), these matrices were as follows:

$$[T] = \begin{bmatrix} 1 & 0 & 0 \\ 1 & 5 & 25 \\ 1 & 10 & 100 \\ 1 & 15 & 225 \\ 1 & 20 & 400 \\ 1 & 25 & 625 \end{bmatrix}; [\Theta] = \begin{bmatrix} 0.821 & 0.321 & 0 & -0.143 & -0.107 & 0.107 \\ -0.118 & 0.001 & 0.066 & 0.077 & 0.035 & -0.061 \\ 0.004 & -0.001 & -0.003 & -0.003 & -0.001 & 0.004 \end{bmatrix};$$

$$[K] = \begin{bmatrix} 385.893 & 5.612 & -0.549 \\ 341.929 & 10.513 & -0.759 \\ 54.857 & -0.903 & 0.057 \end{bmatrix}.$$

After comparing these matrices, it could be concluded that parameters K_{12} and K_{22} were much higher for the elongated counter-rotating stage (D_4 = const). This fact substantiated a decrease in pressure head and power consumption.

The approximating curves evaluated by Formula (4) are presented in Figure 9.

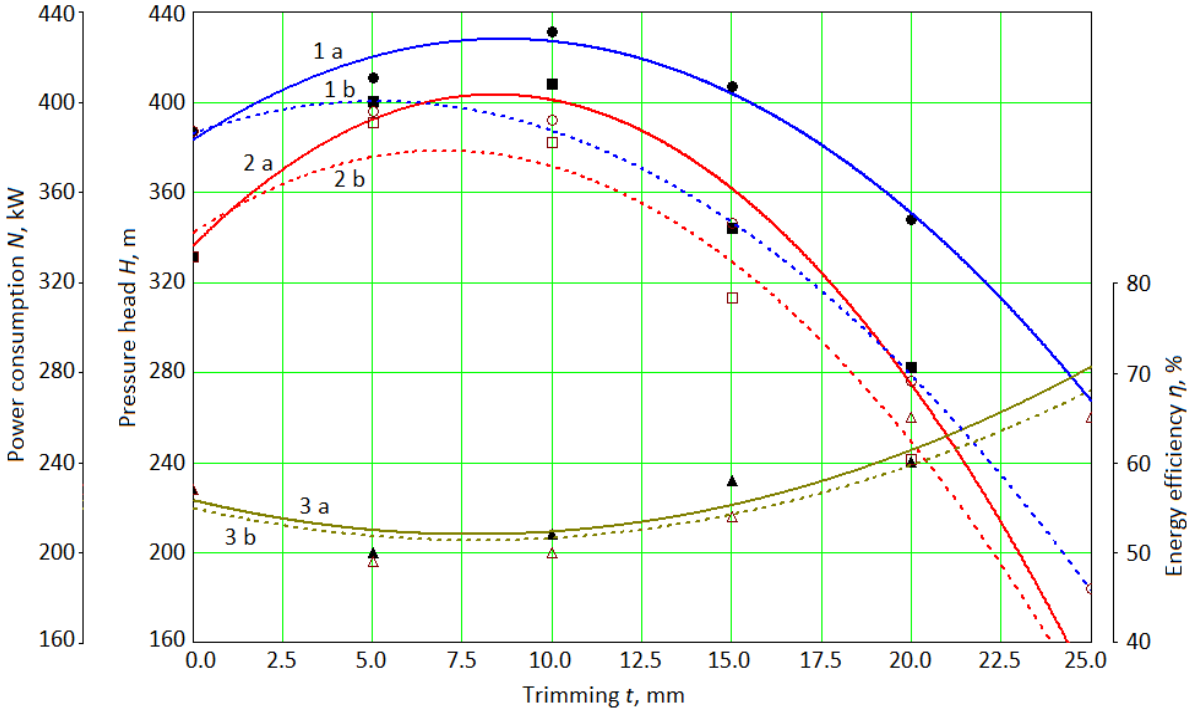

Figure 9. Pressure and energy characteristics for various trimming values: 1—pressure head, m; 2—power consumption, kW; 3—energy efficiency, %; a—the elongated counter-rotating stage (D_4 = const); b—the replaced counter-rotating stage (h = const).

The solid blue line 1a represents the approximating curve for the pressure head for the elongated counter-rotating stage (D_4 = const), shown by filled round dots. The dashed blue line 1b is the approximating curve for the pressure head for the case of the replaced counter-rotating stage (h = const), represented by unfilled round dots. Red curves 2a and 2b represent the power consumption (marked by square dots) for the abovementioned cases. Curves 3a and 3b, marked by the swamp color, approximate the power consumption marked by triangular dots.

Since K_{12} and K_{22} were positive for both cases, the curves of $H(t)$ and $N(t)$ ascended. However, negative values of K_{32} led to a descending angle of energy efficiency $\eta(t)$ for low trimming values. Since K_{13} and K_{23} were negative for both cases, the curves of $H(t)$ and $N(t)$ were convex. However, positive values of K_{33} led to a concave curve of energy efficiency $\eta(t)$.

According to Formulas (10) and (11), the minimum value of energy efficiency η_{min} = 52% corresponded to the trimming of 7.8 mm for the case of the replaced counter-rotating stage (h = const). However, the maximum values of pressure head H_{max} = 428 m and power consumption N_{max} = 403 kW were reached for the trimmings of about 8.5 mm for the case of the elongated counter-rotating stage (D_4 = const).

4. Discussion

After obtaining the pressure and energy characteristics of the counter-rotating stages with different trimmings, the following conclusions were made. They had different pressure characteristics compared to the reference impeller. They could both increase and decrease. Particularly, the pressure head and power consumption increased and reached their maximum for a trimming of about 8 mm. After this, these characteristics decreased.

After comparing two studies (for D_4 = constant and h = constant), the difference in the pressure and energy characteristics could be seen. For the case of D_4 = constant, these characteristics were higher than for the case of h = constant.

On the other hand, for the case of h = constant, the pressure head did not change significantly for trimmings less than 5 mm. However, for higher trimmings, the pressure head decreased significantly.

The energy characteristics also increased for trimmings up to 7–8 mm; however, after this, they decreased too. Due to the high power, the energy efficiency decreased, reaching its minimum at about 7.8 mm, then slowly increased.

After comparing the case of the replaced counter-rotating stage without trimming, the pressure head for trimming about 15 mm was equal to the pressure head of the reference impeller. This fact decreased energy efficiency. Under trimming of about 16 mm, the power consumption would already be the same. In this case, the pressure head and energy efficiency changed.

For the case of the elongated counter-rotating stage, for trimming 15.5 mm, the energy efficiency would be the same as for the impeller without trimming. However, with trimming of about 17 mm, the pressure head and power consumption were the same too. This was the optimal option for trimming, as the power consumed was the same and the pressure was higher compared to the impeller without trimming. In this regard, the main advantage was that the efficiency of the counter-rotating stage increased, and its overall dimensions decreased from 151 mm to 134 mm. This allowed us to reduce the material consumption of the impeller by up to 20%.

The following facts also highlighted the significance of the obtained results. Firstly, when trimming the impeller by 15 mm, the same characteristics as without trimming at a smaller diameter were reached. This led to a smaller diameter of the pumping equipment and reduced material consumption.

Secondly, in [26], an increase in the pressure head of the pump stage occurred due to the improvement of the design of the impeller blade system. The primary disadvantage of that method was the presence of a sinking shape of the head characteristic. This led

to a breakdown of the pump parameters in off-design operation modes. However, the proposed counter-rotating state avoided this problem.

In paper [4], an increase in the pressure head of the pump stage was achieved by changing the width of the inter-vane channel at the outlet. However, this changed the flow rate, which was not satisfactory in the designing of pumping units.

Finally, paper [20] showed that cutting only the impeller's cover disk led to a deterioration in the tangential momentum of the fluid flow at the impeller outlet. Thus, we can conclude that trimming should be performed on both disks simultaneously.

5. Conclusions

It can be concluded that the pressure head is affected not only by trimming, but also by the dimensions of the working part of the impeller. This is because the liquid no longer interacts with the impeller blades and vane disks of larger size.

The counter-rotating effect essentially impacts the pumping unit's pressure and energy characteristics. However, the size and time of interaction of the liquid with the blades also significantly impact the characteristics of the counter-rotating stage.

Relatively low values of impeller trimming increase pressure. However, energy efficiency decreases rapidly. Therefore, impeller trimming is impractical for obtaining higher values of pressure head for the case of a replaced counter-rotating stage. However, impeller trimming is effective for the case of an elongated counter-rotating stage, for which much better characteristics are achieved.

Overall, based on these obtained results, the impeller can be trimmed by 14.0–16.5 mm while maintaining reasonable pressure and energy characteristics.

Further, using pumps with a counter-rotating stage reduces the weight and size indicators of centrifugal pumps and, therefore, their cost. They also allow for reducing radial and axial loads on bearing supports and radial dimensions of the flow parts. Since the obtained results allowed an understanding of the principle of operation for counter-rotating stages, they open ways for further research on variations and technical designs and the possibilities of creating a prototype of the pumping unit so as to test it in practice.

Author Contributions: Conceptualization, O.K. and O.R.; methodology, I.P. and O.K.; software, V.I.; validation, J.P.; formal analysis, V.I. and V.K.; investigation, O.K. and O.R.; resources, I.P. and J.P.; data curation, V.K.; writing—original draft preparation, I.P.; writing—review and editing, V.I.; visualization, V.K.; supervision, O.R.; project administration, I.P.; funding acquisition, J.P. All authors have read and agreed to the published version of the manuscript.

Funding: This work was supported by the project "Development of excellent research capacities in the field of additive technologies for the Industry of the 21st century", ITMS: 313011BWN5, co-financed by the Operational Program Integrated Infrastructure funded by the ERDF, and by the project VEGA 1/0704/22 granted by the Ministry of Education, Science, Research and Sport of the Slovak Republic.

Institutional Review Board Statement: Not applicable.

Informed Consent Statement: Not applicable.

Data Availability Statement: The data presented in this study are available on request from the corresponding author.

Acknowledgments: The research was partially carried out within the R&D project "Ensuring energy efficiency and vibration reliability of rotary machines" of the National Scholarship Programme of the Slovak Republic, supported by the Slovak Academic Information Agency (SAIA, n.o.). The results were also partially obtained within the Ulam NAWA Programme, grant number BPN/ULM/2022/1/00042. The authors acknowledge the International Association for Technological Development and Innovations for support while conducting the research.

Conflicts of Interest: The authors declare no conflict of interest.

References

1. Zhou, P.; Tang, J.; Mou, J.; Zhu, B. Effect of impeller trimming on performance. *World Pumps* **2016**, *2016*, 38–41. [CrossRef]
2. Savar, M.; Kozmar, H.; Sutlovic, I. Improving centrifugal pump efficiency by impeller trimming. *Desalination* **2009**, *249*, 654–659. [CrossRef]
3. Mandryka, A.; Majid, A.P.; Ratushnyi, O.; Kulikov, O.; Sukhostavets, D. Ways for improvement of reverse axial pumps. *J. Eng. Sci.* **2022**, *9*, D14–D19. [CrossRef]
4. Li, W.-G. Impeller trimming of an industrial centrifugal viscous oil pump. *Int. J. Adv. Des. Manuf. Technol.* **2011**, *5*, 1–10.
5. Detert Oude Weme, D.G.J.; van der Schoot, M.S.; Kruyt, N.P.; van der Zijden, E.J.J. Prediction of the effect of impeller trimming on the hydraulic performance of low specific-speed centrifugal pumps. *J. Fluids Eng.* **2018**, *140*, 081202. [CrossRef]
6. Khoeini, D.; Tavakoli, M.R. Flow characteristics of a centrifugal pump with different impeller trimming methods. *FME Trans.* **2018**, *46*, 463–468. [CrossRef]
7. Deng, Q.; Pei, J.; Wang, W.; Yuan, S. Effects of impeller trimming on performance in a double-suction centrifugal pump. *IOP Conf. Ser. Earth Environ. Sci.* **2021**, *627*, 012014. [CrossRef]
8. Deng, Q.; Pei, J.; Wang, W.; Lin, B.; Zhang, C.; Zhao, J. Energy loss and radial force variation caused by impeller trimming in a double-suction centrifugal pump. *Entropy* **2021**, *23*, 1228. [CrossRef]
9. Swain, D.; Engeda, A. Performance impact of impeller blade trimming on centrifugal compressors. *Proc. Inst. Mech. Eng. Part A J. Power Energy* **2014**, *228*, 878–888. [CrossRef]
10. Jawad, L.H.; Abdullah, S.; Zulkifli, R.; Mahmood, W.M.F.W. Numerical investigation on the effect of impeller trimming on the performance of a modified compressor. *CFD Lett.* **2013**, *5*, 174–184.
11. Yang, S.-S.; Kong, F.-Y.; Jiang, W.-M.; Qu, X.-Y. Effects of impeller trimming influencing pump as turbine. *Comput. Fluids* **2012**, *67*, 72–78. [CrossRef]
12. Yang, S.; Shao, K.; Dai, T. Influence of parallel impeller inlet trimming on mixed flow pump as turbine. *J. Shanghai Jiaotong Univ.* **2020**, *54*, 805–812. [CrossRef]
13. Wang, K.; Ju, Y.; Zhang, C. Experimental and numerical investigations on effect of blade trimming on aerodynamic performance of squirrel cage fan. *Int. J. Mech. Sci.* **2020**, *177*, 105579. [CrossRef]
14. Li, C.; Li, X.; Li, P.; Ye, X. Numerical investigation of impeller trimming effect on performance of an axial flow fan. *Energy* **2014**, *75*, 534–548. [CrossRef]
15. Ye, X.; Ding, X.; Li, C. Performance and static analysis of an axial fan after blade trimming. *J. Chin. Soc. Power Eng.* **2015**, *35*, 752–759.
16. Shi, C.; Chai, S.; Di, L.; Ji, C.; Ge, Y.; Wang, H. Combined experimental-numerical analysis of hydrogen as a combustion enhancer applied to Wankel engine. *Energy* **2023**, *263*, 125896. [CrossRef]
17. Shi, C.; Zhang, P.; Ji, C.; Di, L.; Zhu, Z.; Wang, H. Understanding the role of turbulence-induced blade configuration in improving combustion process for hydrogen-enriched rotary engine. *Fuel* **2022**, *319*, 123807. [CrossRef]
18. Bao, J.; Qu, P.; Wang, H.; Zhou, C.; Zhang, L.; Shi, C. Implementation of various bowl designs in an HPDI natural gas engine focused on performance and pollutant emission. *Chemosphere* **2022**, *303*, 135275. [CrossRef]
19. Qu, X.; Wang, L. Effects of impeller trimming methods on performances of centrifugal pump. *J. Energy Eng.* **2016**, *142*, 343. [CrossRef]
20. Shadab, M.; Karimipour, M.; Najafi, A.F.; Paydar, R.; Nourbakhsh, S.A. Effect of impeller shroud trimming on the hydraulic performance of centrifugal pumps with low and medium specific speeds. *Eng. Appl. Comput. Fluid Mech.* **2022**, *16*, 514–535. [CrossRef]
21. Ciocanea, A. Method for mitigating the negative effect of vortex motion inside the suction chambers of centrifugal pumps. *INCAS Bull.* **2013**, *5*, 37–44. [CrossRef]
22. Reza, F.-A.; Babak, L.-A.; Alireza, K. On the measurement of ram-pump power by changing in water hammer pressure wave energy. *Ain Shams Eng. J.* **2019**, *10*, 681–693. [CrossRef]
23. Baha, V.; Lishchenko, N.; Vanyeyev, S.; Mižáková, J.; Rodymchenko, T.; Piteľ, J. Numerical simulation of gas flow passing through slots of various shapes in labyrinth seals. *Energies* **2022**, *15*, 2971. [CrossRef]
24. Pavlenko, I.; Kuric, I.; Basova, Y.; Saga, M.; Ivanov, V.; Kotliar, A.; Trojanowska, J. Parameter identification of a disscrete-mass mathematical model of crankshaft oscillations. *J. Braz. Soc. Mech. Sci. Eng.* **2022**, *44*, 601. [CrossRef]
25. Zawawi, M.H.; Saleha, A.; Salwa, A.; Hassan, N.H.; Zahari, N.M.; Ramli, M.Z.; Muda, Z.C. A review: Fundamentals of computational fluid dynamics (CFD). *AIP Conf. Proc.* **2018**, *2030*, 020252. [CrossRef]
26. Kondus, V.; Gusak, O.; Yevtushenko, Y. Investigation of the operating process of a high-pressure centrifugal pump with taking into account of improvement the process of fluid flowing in its flowing part. *J. Phys. Conf. Ser.* **2021**, *1741*, 012012. [CrossRef]